This is a repository copy of *Droplet epitaxy of InAs/InP quantum dots via MOVPE by using an InGaAs interlayer*.

White Rose Research Online URL for this paper:
https://eprints.whiterose.ac.uk/180955/

Version: Published Version

Article:

Sala, D.E.M., Godsland, M., Na, Y.I. et al. (2 more authors) (2021) Droplet epitaxy of InAs/InP quantum dots via MOVPE by using an InGaAs interlayer. Nanotechnology, 33 (6). 065601. ISSN 0957-4484

https://doi.org/10.1088/1361-6528/ac3617

Reuse
This article is distributed under the terms of the Creative Commons Attribution (CC BY) licence. This licence allows you to distribute, remix, tweak, and build upon the work, even commercially, as long as you credit the authors for the original work. More information and the full terms of the licence here:
https://creativecommons.org/licenses/

Takedown
If you consider content in White Rose Research Online to be in breach of UK law, please notify us by emailing eprints@whiterose.ac.uk including the URL of the record and the reason for the withdrawal request.

eprints@whiterose.ac.uk
https://eprints.whiterose.ac.uk/

Nanotechnology

PAPER • OPEN ACCESS

Droplet epitaxy of InAs/InP quantum dots via MOVPE by using an InGaAs interlayer

To cite this article: Elisa M Sala *et al* 2022 *Nanotechnology* **33** 065601

View the article online for updates and enhancements.

You may also like

- A Viable Route to Enhance Permittivity of Gate Dielectrics on $In_{0.53}Ga_{0.47}As(001)$: Trimethylaluminum-Based Atomic Layer Deposition of MeO_2 (Me = Zr, Hf)
  A. Molle, E. Cianci, A. Lamperti et al.
- Effect of high-pressure deuterium annealing with high- stack onto $In_{0.53}Ga_{0.47}As$ MOS capacitors on 300 mm Si substrate
  Seung Heon Shin, Dae-Hyun Kim and Tae-Woo Kim
- Atomic Layer Deposition of Al-Doped ZrO_2 Thin Films as Gate Dielectric for $In_{0.53}Ga_{0.47}As$
  L. Lamagna, A. Molle, C. Wiemer et al.

The Electrochemical Society
Advancing solid state & electrochemical science & technology
241st ECS Meeting
May 29 – June 2, 2022 Vancouver • BC • Canada
Extended abstract submission deadline: **Dec 17, 2021**
Connect. Engage. Champion. Empower. Acclerate.
Move science forward

Submit your abstract

This content was downloaded from IP address 86.145.241.120 on 29/11/2021 at 12:15

OPEN ACCESS
IOP Publishing

Nanotechnology

Nanotechnology **33** (2022) 065601 (8pp)

https://doi.org/10.1088/1361-6528/ac3617

Droplet epitaxy of InAs/InP quantum dots via MOVPE by using an InGaAs interlayer

Elisa M Sala[1,2], Max Godsland[2], Young In Na[2], Aristotelis Trapalis[1,2] and Jon Heffernan[1,2]

[1] EPSRC National Epitaxy Facility, The University of Sheffield, North Campus, Broad Lane, S3 7HQ Sheffield, United Kingdom
[2] Department of Electronic and Electrical Engineering, The University of Sheffield, North Campus, Broad Lane, S37HQ Sheffield, United Kingdom

E-mail: e.m.sala@sheffield.ac.uk

Received 30 July 2021, revised 29 October 2021
Accepted for publication 3 November 2021
Published 19 November 2021

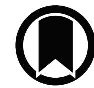

Abstract

InAs quantum dots (QDs) are grown on an $In_{0.53}Ga_{0.47}As$ interlayer and embedded in an InP (100) matrix. They are fabricated via droplet epitaxy (DE) in a metal organic vapor phase epitaxy (MOVPE) reactor. Formation of metallic indium droplets on the $In_{0.53}Ga_{0.47}As$ lattice-matched layer and their crystallization into QDs is demonstrated for the first time in MOVPE. The presence of the $In_{0.53}Ga_{0.47}As$ layer prevents the formation of an unintentional non-stoichiometric 2D layer underneath and around the QDs, via suppression of the As-P exchange. The $In_{0.53}Ga_{0.47}As$ layer affects the surface diffusion leading to a modified droplet crystallization process, where unexpectedly the size of the resulting QDs is found to be inversely proportional to the indium supply. Bright single dot emission is detected via micro-photoluminescence at low temperature, ranging from 1440 to 1600 nm, covering the technologically relevant telecom C-band. Transmission electron microscopy investigations reveal buried quantum dots with truncated pyramid shape without defects or dislocations.

Keywords: MOVPE, droplet epitaxy, III–V quantum dots, AFM, photoluminescence, TEM

(Some figures may appear in colour only in the online journal)

1. Introduction

In the last decade, III–V quantum dots (QDs) fabricated by droplet epitaxy (DE) have attracted great interest due to their suitability for a wide range of applications, ranging from quantum photonics, where they can be employed as efficient quantum emitters of single and entangled photon pairs [1], to photodetectors [2], lasers [3], and solar cells [4]. DE is a flexible growth technique for the fabrication of QDs compared to the alternative Stranski–Krastanow (SK) method which has been extensively used to grow strain-driven self-assembled QDs [5–8]. Since DE does not depend on strain in the system, there is an added degree of freedom to pursue QD formation on different substrates. Moreover, DE also enables the technique of local droplet etching [1, 9, 10] which is then used as a template for site-controlled QD formation [11, 12]. Among others, InAs/InP QDs fabricated by DE in MOVPE were successfully used as building blocks for the first quantum light emitting diode (QLED) emitting at 1.5 μm [13] and enabled teleportation of qubits [14, 15]. Also, very recently DE in combination with droplet etching of InAs/InP QDs emitting at the telecom C-band has been demonstrated [16] and [25], showing an additional and promising approach for nanostructure tuning during MOVPE growth. Such QDs can be employed as fundamental units for the fast-developing quantum information technology, particularly for quantum networks [17–19]. Additional promising design strategies include, for instance, embedding InAs QDs in an InGaAs quantum well (QW). This allowed for an efficient post-growth tuning of the QD emission in the telecom O-band via the quantum-confined Stark effect in an entangled light emitting diode (ELED) [17]. Therefore, such strategy can be applied also

Original content from this work may be used under the terms of the Creative Commons Attribution 4.0 licence. Any further distribution of this work must maintain attribution to the author(s) and the title of the work, journal citation and DOI.

to QDs emitting at the low-loss telecom C-band, and thus combining the use of a QW underneath the QDs with DE QDs is a promising approach.

In this letter, we demonstrate the growth of InAs QDs on an $In_{0.53}Ga_{0.47}As$ lattice-matched layer to InP(100), using DE in MOVPE. Indium droplet deposition and InAs QDs formation are studied. The QDs are characterized morphologically by atomic force microscopy (AFM) and transmission electron microscopy (TEM), and optically via macro photoluminescence at room-temperature (RT-PL) and micro-PL at low-temperature (LT-μPL). Deposition of indium droplets on $In_{0.53}Ga_{0.47}As$ and their crystallization into dots [20] or rings [21] have been investigated only in a limited manner under MBE conditions. Studies of InAs QDs growth on graded $In_{0.53-0.72}Ga_{0.47-0.28}As/InP$ [22] and lattice-matched $In_{0.53}Ga_{0.47}As/InP$ [23, 24] in MOVPE can be also found, where the InAs dots were fabricated by SK [24] or atomic layer epitaxy (ALE) methods [22, 23], using N_2 as carrier gas instead of H_2. To our knowledge, this is the first report of the use of this approach with DE by MOVPE.

2. Sample fabrication

The samples studied in this work were grown in a 3 × 2 close-coupled showerhead (CCS) Aixtron reactor using H_2 as a carrier gas. The group-V precursor materials used are arsine (AsH_3) and phosphine (PH_3), and for group-III trymethylindium (TMIn) and trymethylgallium (TMGa). First, a ∼300 nm InP buffer is grown on InP (100) at a substrate temperature of 600 °C, and a 5 nm $In_{0.53}Ga_{0.47}As$ layer lattice-matched to InP is deposited on top of it. In order to study indium droplet formation and crystallization into InAs QDs, the temperature is lowered to a range of 320 °C–400 °C for droplet deposition and afterwards indium is supplied with a constant flow of 1.4 μmol min^{-1}, for times between 15 and 35 s. With the first set of samples, we investigated the droplet formation on the $In_{0.53}Ga_{0.47}As$ surface. Thus, after indium deposition and droplet formation, the samples are cooled down and removed from the reactor. For QD formation the droplets are exposed to an Arsenic flow of 24 μmol min^{-1} while ramping the temperature up to 520 °C, as carried out in our previous works on InP [16, 25]. We note that the end temperature of 520 °C was the optimum temperature yielding high-quality InAs QDs in our previous experiments [16, 25]. The QDs are then capped with 20 nm InP grown at 520 °C, and an additional InP layer ∼80 nm thick is grown on top, at a higher temperature of ∼600 °C to fully bury the QDs. In order to morphologically investigate uncapped QDs with AFM, the structure was completed with additional InGaAs and a surface QD layer grown following the same procedure outlined above. The samples were then immediately cooled down and removed from the growth chamber for *ex situ* characterizations.

3. Structural and optical investigation via AFM and PL

With the set of indium droplet samples, we investigated the morphology of droplets on the 5 nm $In_{0.53}Ga_{0.47}As$ layer via AFM, and compared the differences with their formation on bare InP as reported in our previous work [16]. Figure 1 displays AFM micrographs of $In_{0.53}Ga_{0.47}As/InP$ surfaces where indium droplets were deposited at a temperature varying between 320 °C and 400 °C, alongside the respective surface profiles of selected areas [26]. As one can clearly see, starting from 400 °C, round symmetrically shaped droplets form, while at lower temperatures the indium apparently wets homogeneously the $In_{0.53}Ga_{0.47}As$ surface but no droplets are detected. Also, regular monolayer-steps typical of a step-flow growth are observed, without cluster formation. Profiles of figures 1(a) and (b) show a similar root mean square (rms) roughness of about 0.2 nm and no macroscopic indium droplets can be detected. In contrast, on a bare InP (100) surface, round-shaped indium droplets always nucleate as long as the TMIn is fully cracked, even at a substrate temperature as low as ca. 300 °C, as we previously reported [16]. Here, the growth of the InGaAs layer appears to have modified the surface diffusion of indium adatoms, thus affecting the formation of macroscopic indium droplets. In fact, as reported by Stevens *et al* [20], the activation energy E_A and the diffusivity prefactor D_0 of indium on an $In_{0.53}Ga_{0.47}As$ surface are greater than the ones of a bare InP, on both crystallographic directions [011] and [0–11]. This means that a higher substrate temperature is needed for the indium to become mobile enough to coalesce and form detectable droplets. Indeed, when the surface temperature is raised up to 400 °C, droplets can be clearly observed, see figure 1 (c).

The distribution of droplet sizes is presented in figure 2 below, showing (a) variable diameters ranging from 15 to 55 nm and (b) heights from 2 to 20 nm [26]. Providing the same growth conditions [16], on bare InP the indium droplets were bigger, showing generally more homogeneous size distributions, e.g. heights in the range of 39–45 nm and widths of 68–80 nm, as shown by the purple histograms of figures 2(a), (b). This is again most likely a result of the reduced surface diffusion of indium on InGaAs, as discussed above. Also, the total droplet density here is $\sim 3 \cdot 10^8$ cm^{-2}, higher compared to the $\sim 6 \cdot 10^7$ cm^{-2} found previously [16].

In order to form InAs QDs, the indium droplets are exposed to an Arsenic flow, while ramping the temperature to 520 °C [16]. Figures 3(a)–(d) shows AFM micrographs of InGaAs/InP surfaces with varying indium supply for QD formation [26]. Here, we study the QD formation depending on the indium supply: the indium flow has been kept constant, while the deposition time has been varied between 15 and 35 s. For 15 s, no QDs can be observed, as seen in figure 3(a), and the surface presents an rms of ca. 0.2 nm. When the indium deposition time is increased, QDs can be detected, see figures 3(c)–(d). Counterintuitively, and different to what is typically found in SK QDs [5], first bigger QDs form and only after further increasing the supplied indium amount, smaller QDs form. In fact, the QD formation here is not driven by strain, as in SK, but relies on the nucleation of indium droplets at first instance, and the final dot density strongly depends on the indium mobility on the surface. Compared to bare InP, here the surface diffusion of indium on InGaAs is reduced, leading to the nucleation of larger QDs first. QDs show density of $\sim 6 \cdot 10^8$ cm^{-2}, $\sim 4 \cdot 10^9$ cm^{-2}, and $\sim 1 \cdot 10^{10}$ cm^{-2}, for an indium amount of 20, 25 and 35 s, respectively. It

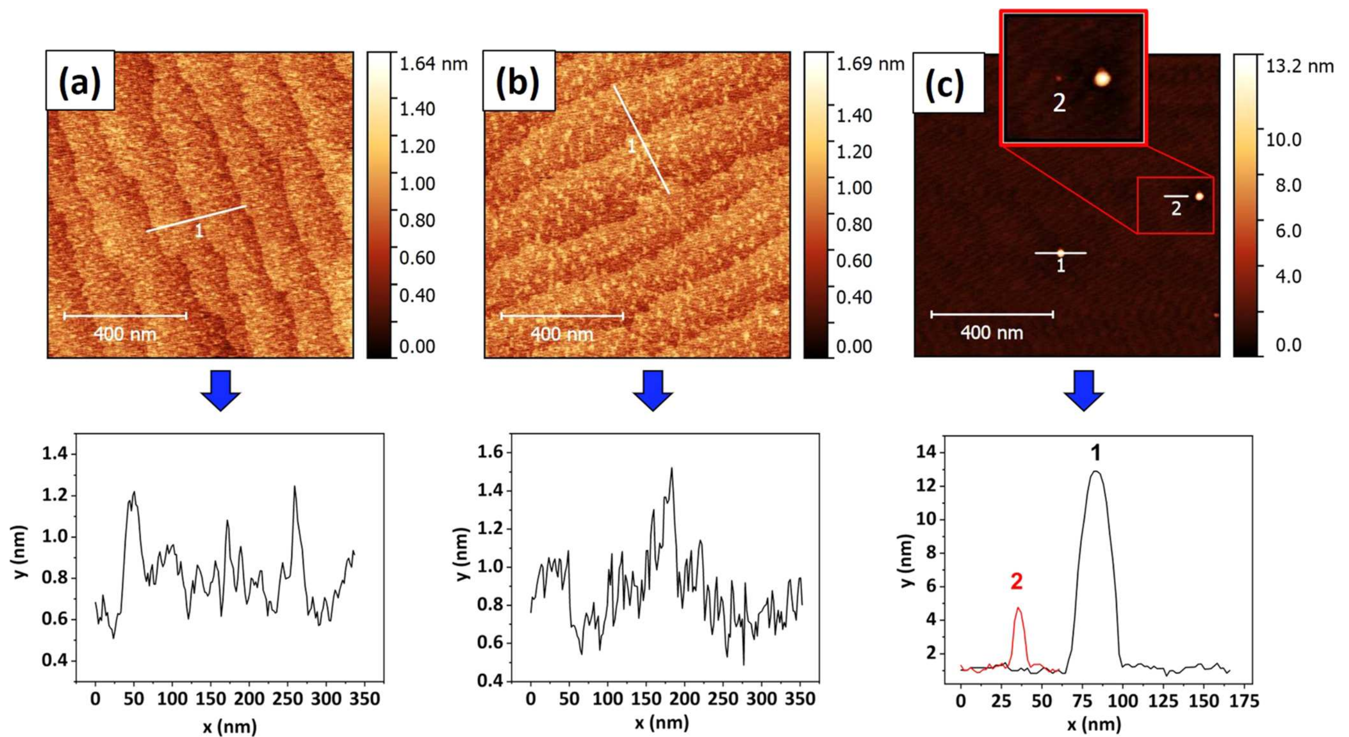

Figure 1. AFM micrographs of the 5 nm $In_{0.53}Ga_{0.47}As/InP$ surface after 35 s long deposition of indium with increasing temperatures: (a) 320 °C, (b) 350 °C, (c) 400 °C. Inset in (c) shows the magnification of the region containing the small droplet 2 [26].

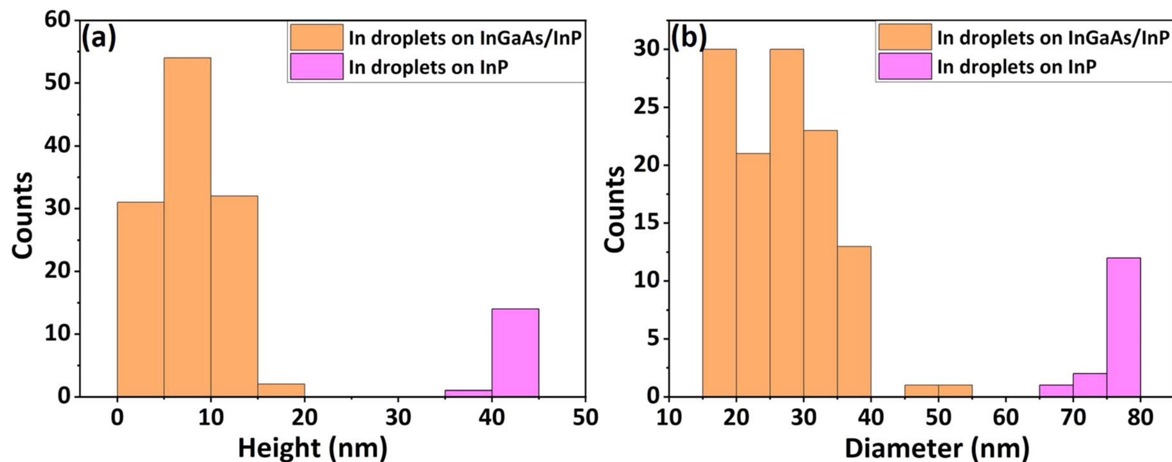

Figure 2. Distribution of heights (a) and diameters (b) of indium droplets deposited at 400 °C, for two different surfaces: on the InGaAs layer (orange) and on bare InP (purple) [26].

is worth noticing that, unlike in our previous investigations of InAs DE QDs on bare InP [16], such QD density is up to 2 orders of magnitude higher than the initial droplets ($\sim 3 \cdot 10^8$ cm^{-2}). This suggests that some of the indium wetting the InGaAs surface coalesces and gets crystallized during the temperature ramping step and As supply step. Most likely, the increase in temperature during the ramp gradually enhances the indium mobility, so that it can coalesce and become crystallized.

Figures 4(a) and (b) show QD size distribution as a function of deposited indium. QDs have a mean diameter of (53 ± 21) nm, (47 ± 16) nm, and (41 ± 21) nm, for samples grown with 20, 25 and 35 s, respectively [26]. Corresponding height distributions are: (9.2 ± 1.7), (6.2 ± 1.7), and (5.4 ± 2) nm.

Optical investigations of the QDs have been carried out, by means of RT-PL and LT-μPL. All samples investigated in this work with RT-PL have been excited with a 645 nm diode laser with an ∼85 W cm^{-2} power density. Figure 5 shows RT-PL of QDs grown with varying indium deposition time [26]. Here, we assign the emission around 900 nm to the InP substrate [27], the peak around 1.5 μm to the InGaAs layer [28], whilst the peak at longer wavelengths arises from the QDs. The sample with 15 s indium presents only the sharp emission from the InGaAs layer, confirming the absence of QD formation for this time as observed in the AFM investigations of figure 3(a). With increasing indium, long-wavelength emission emerges in the range 1.6–2.4 μm.

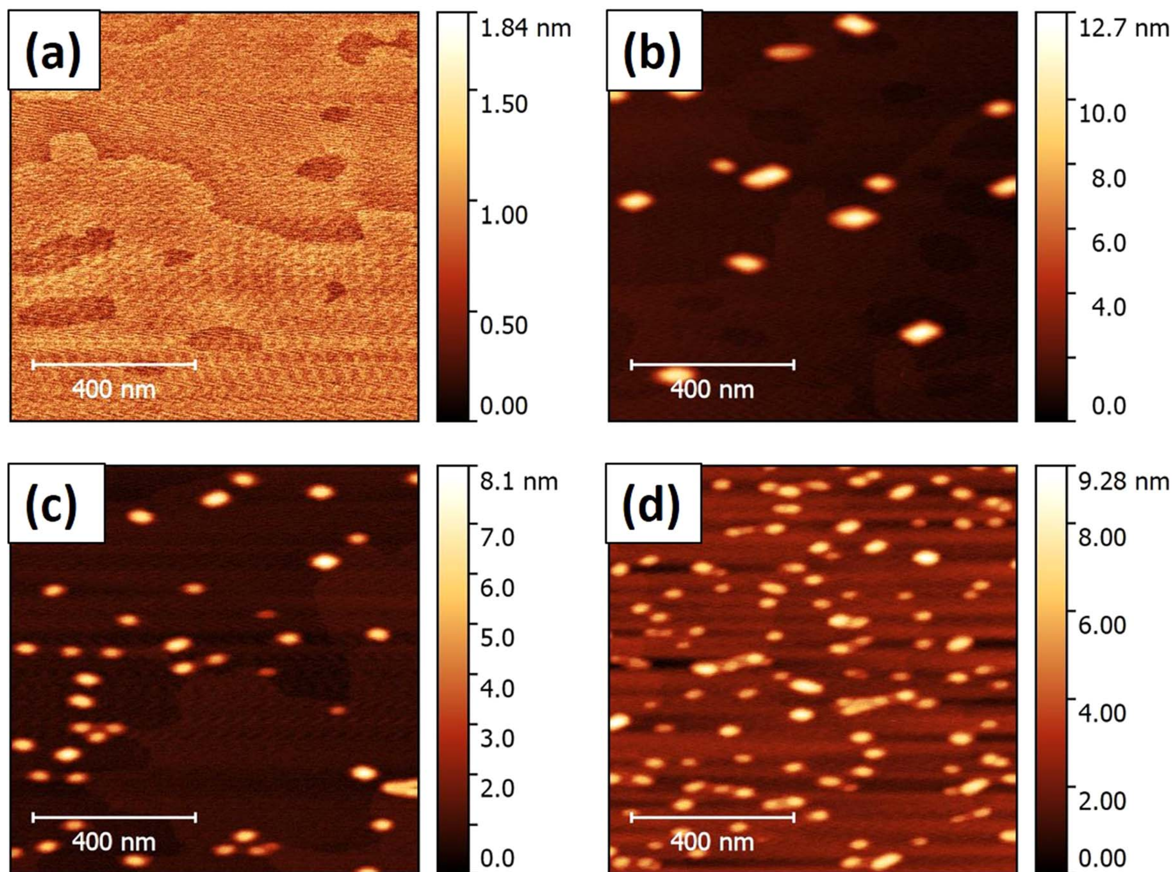

Figure 3. AFM micrographs of uncapped InAs QDs deposited on 5 nm $In_{0.53}Ga_{0.47}As$ interlayer at 400 °C with varying indium deposition time: (a) 15 s, (b) 20 s, (c) 25 s, and (d) 35 s [26].

Interestingly, for 20 s indium, the QD emission lies at the longest wavelengths up to ca. 2.4 μm, suggesting a contribution of larger QDs [29]. In fact, this sample has shown the presence of the largest QDs among all investigated samples in the AFM characterization. With increasing indium supply, the QD-PL shortens to 1.9 and 1.84 μm for 25 and 35 s In, respectively, reflecting a contribution of optically active smaller QDs. The intensity of the QD-PL increases according to the QD density, especially for 35 s In. Comparing the PL signal of these QDs with InAs QDs grown directly on InP [16], we find that the intensity is 3-times greater for the present QDs grown on the InGaAs layer. We believe that (i) this is due to a higher QD density reached by using InGaAs, and (ii) there is no formation of optically active and non-stoichiometric In(As,P) 2D quasi wetting layer (WL) [16, 25] since it is an Arsenic terminated surface that is exposed during the crystallization step, as opposed to the Phosphorous-terminated surface in the case of QDs directly on InP.

To confirm the assignement of the RT-PL peaks, we also carried out LT-μPL characterizations at 4 K on all QD samples using a 635 nm laser, with a power density of 4.5 W cm^{-2}, and a spectrometer with 25 μeV resolution. The μPL spectra were performed on QD ensembles with a collection area of approximately 5 μm in diameter. The measurements are shown in figure 6, alongside the linewidth and emission wavelength distributions. Here, bright and narrow emission lines from single QDs can be detected, ranging between 1440 and 1600 nm, thus including the relevant telecom C-band. The analysis of the wavelength distributions show single and bimodal distributions with increasing indium deposition as follows: single with (1551.1 $\pm$ 27.8) nm for 25, and bimodal with (1490.3 $\pm$ 38.7) nm and (1560.2 $\pm$ 40.7) nm for 35 s. The bimodal wavelength distribution of the 35 s sample reflects the increased contribution to the emission of QDs with a smaller size, as has been observed in figure 3(d). The linewidth distributions measured in these samples were (119 $\pm$ 18) μeV and (130 $\pm$ 24) μeV for 25 and 35 s, respectively. We note here that the measured linewidths are relatively broad (>100 μeV). We suggest that the high density of the QDs and potential defect states in their immediate environment cause an electric field which broadens the single dot emission [30].

Finally, figure 7 shows μPL measurements of the 20 s sample, taken at two different locations on the sample [26]. Here, no sharp single QD lines can be observed, but only much broader emissions. Most likely, this is due to the larger size of the QDs, which could lead to additional charge noise and thus to a considerable broadening of the single dot emission [31].

4. TEM investigations

All samples have been investigated with TEM, in order to have a better insight into the layer structure and buried QDs.

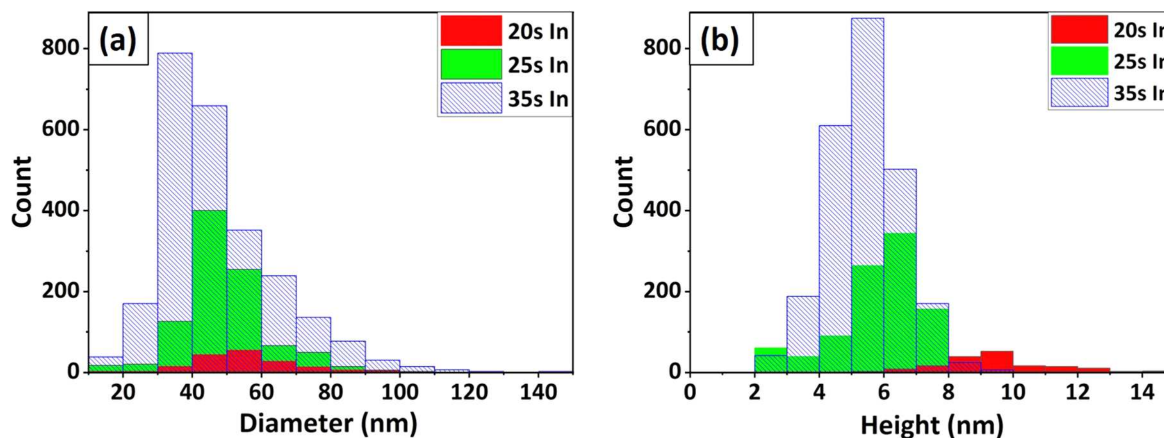

Figure 4. Distribution of diameters (a) and heights (b) of $InAs/In_{0.53}Ga_{0.47}As/InP$ QDs with varying indium deposition time [26].

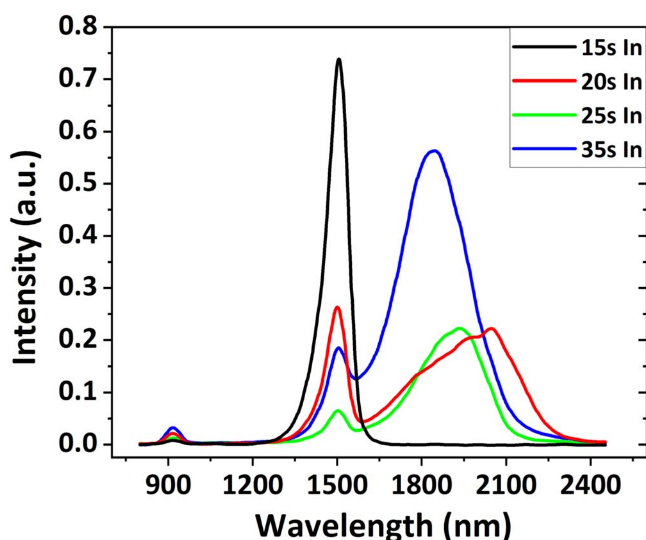

Figure 5. RT-PL measurements of QD samples with varying indium deposition time [26].

TEM measurements have been carried out under dark field (002) diffraction conditions. These conditions are compositionally sensitive, allowing to distiguish the layers of different materials via dark/bright contrast. They are also partially sensitive to strain fields [32]. Figure 8 shows TEM micrographs of all analyzed samples [26]. Figure 8(a) shows a single thick dark line which we ascribe to the As-rich InGaAs layer, emerging against the brighter InP background. The measured thickness of this layer amounts to (5 ± 0.5) nm, in very good agreement with the expected value, thus demonstrating an excellent control on the MOVPE growth process. Here, no QDs can be observed, which is in agreement with the previous findings, where no QDs were detected in AFM, nor evidence of their optical emission could be observed in PL, showing only the bright emission of the InGaAs layer. Figures 8(b) and (c) show two TEM micrographs of the 20 s In sample measured in two different regions. In the region (b), only the InGaAs layer with no buried QDs are detected, but an uncapped QD can be clearly seen on the surface, highlighted with a red dotted line. Instead, in region (c), a buried QD is observed, also highlighted with a red line. It is important to point out that the uncapped QD has a pyramidal shape, while the buried one is a truncated pyramid: this is consistent with what one would expect for buried QDs, since the capping process leads to shape transitions from pyramid to truncated pyramid [5, 33]. The surface QD has base length of ~61 nm and height of ~11 nm, while the buried QD is 50 nm wide and 9 nm height. Figures 8(d) and (e) show buried QDs of samples grown with 25 and 35 s In, respectively. The QDs in such samples show similar truncated-pyramid morphology. **QD-1** in figure 8(d) shows a base length of ~32 nm and a height of ~3.5 nm, while **QD-2** has a base of ~27 nm and a height of ~2.8 nm. QDs in figure 8(e) are the flattest, as also previously observed via AFM investigations. The three highlighted QDs show a base length ranging between 30 and 40 nm and a height of 2–3 nm. The QD dimensions extracted from TEM are in accordance with the AFM data, with heights of the buried QDs slightly reduced, since the buried QDs undergo shape transitions by losing their apex, and thus to a height reduction [33]. In figure 8(d) some diffused areas can be observed, especially for **QD-1**. These are ascribed to strain contrast, resulting from the bending of the (002) diffracted planes [32]. Compared to our previous TEM investigations on InAs QDs on bare InP [25], where such strained areas were more evident, here the contrast appears strongly reduced, if not absent for most of the QDs. This is likely due to the reduced size of these InAs/InGaAs QDs compared to InAs QDs grown on bare InP, considering the same InP cap thickness of 20 nm [16, 25].

The homogeneous contrast in the region above the QDs suggests that material intermixing can be excluded. It is also worth noting that the InGaAs layer has a comparable thickness for all investigated samples, and it presents an homogeneous dark contrast emerging from the brighter background, suggesting an homogeneous composition. There is no evidence from our TEM investigations, nor from the PL, of an additional InAs wetting layer. The TEM also confirms that, compared to InAs DE QDs grown directly on InP [16, 25], the presence of the InGaAs layer prevented the formation of the non-stoichiometric 2D In(As,P) quasi-wetting layer [16, 25]. This is an important advantage to the use of an InGaAs interlayer which effectively suppresses the As/

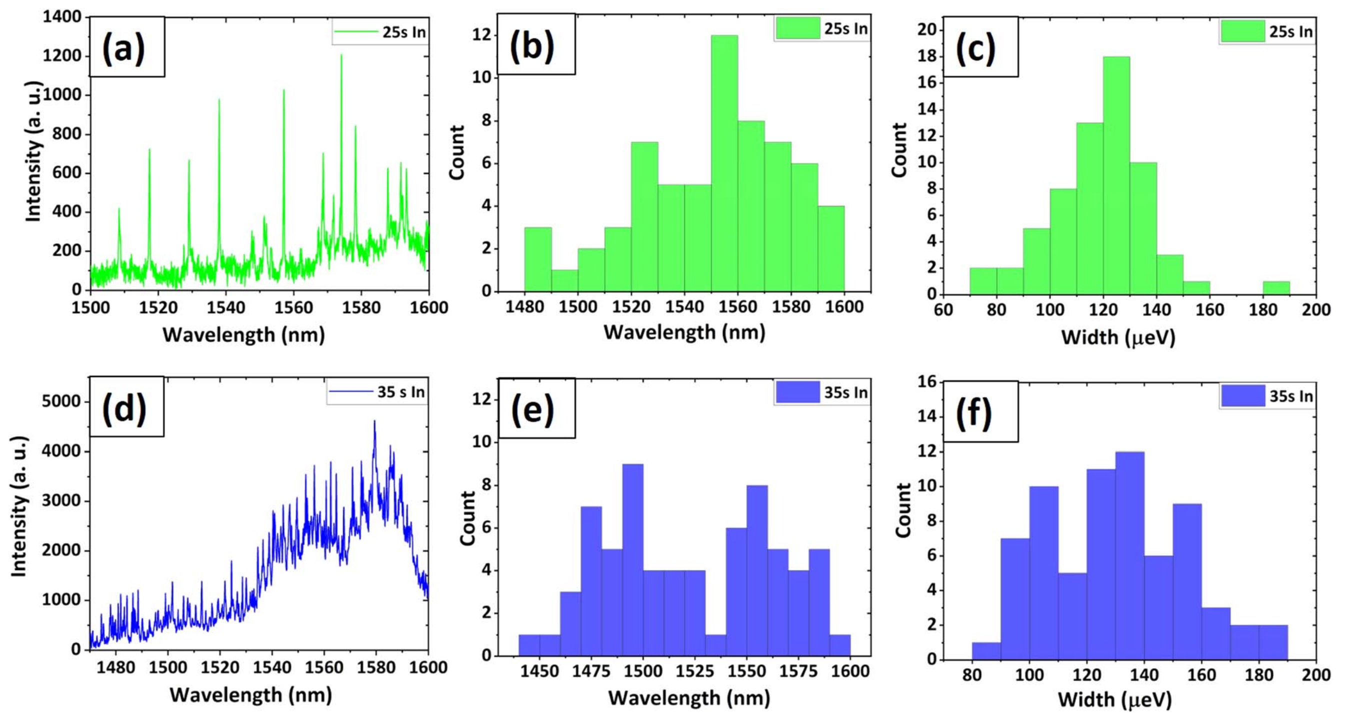

Figure 6. μPL characterizations carried out at 4K alongside the linewidth and wavelength distributions, of samples grown with (a)–(c) 25 s and (d)–(f) 35 s indium deposition time. Same color scale used as in figures 4 and 5 [26].

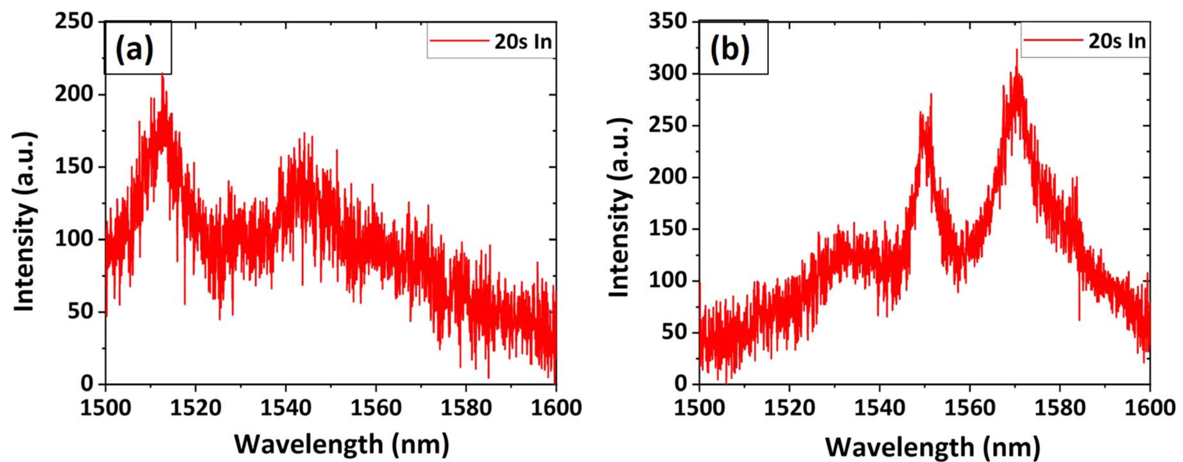

Figure 7. μPL characterizations carried out at 4K of the sample grown with 20 s indium deposition time, recorded at two different locations (a) and (b). Same color scale as previously used [26].

P exchange during dot crystallization by isolating the InAs QDs from the InP surface. Finally, we note that in all samples no detectable defects or dislocations can be found, pointing to a very good crystal quality.

5. Conclusions

In conclusion, we have investigated the growth of InAs QDs by droplet epitaxy in a MOVPE environment, for the first time on an $In_{0.53}Ga_{0.47}As$ layer lattice-matched to InP. We have shown that the formation of indium droplets appears to be strongly affected by the presence of the interlayer, which modifies the indium surface diffusion. This leads to formation of smaller droplets, compared to that on bare InP [25]. Additionally, the modification of the surface diffusion leads to a modified crystallization process of indium droplets into InAs QDs, where first bigger QDs form and, with increasing indium amount, crystallization of smaller QDs occurs. Growing the QDs on such an interlayer allowed us to sucesfully suppress the formation of the unintentional non-stoichiometric In(As,P) 2D layer, previously observed for the InAs QDs grown directly on InP [16, 25]. This is due to the ‘isolation’ between the InP matrix and the InAs QDs provided by the InGaAs layer, leading to the suppression of the As–P exchange reactions during the droplet crystallization into InAs QDs. Low temperature μPL reveals emission from single QDs, ranging from 1450 to 1600 nm, covering the

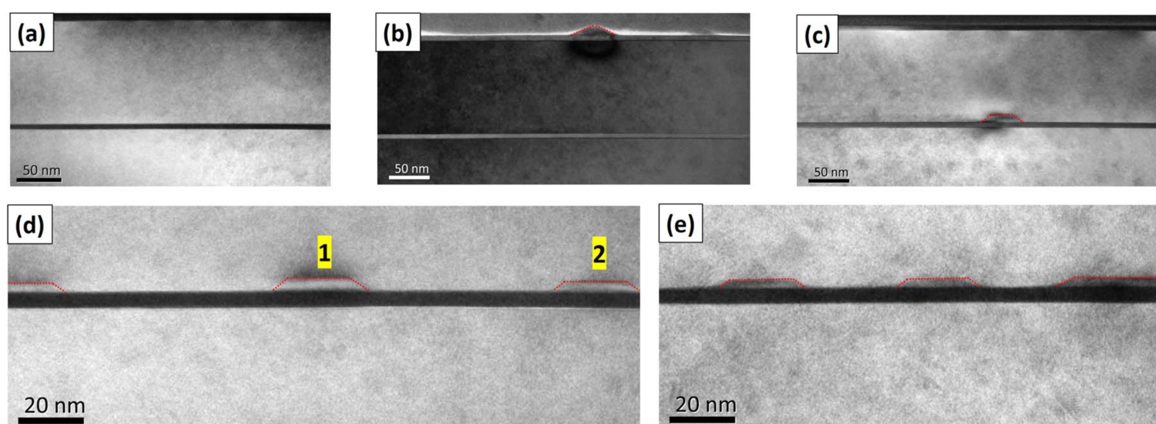

Figure 8. TEM micrographs of samples (a)–(e). QDs are highlighted with red dotted lines as a guide for the eye [26].

technologically relevant telecom C-band. We note that such InAs/InGaAs/InP QDs present a comparable or superior brightness and a similar linewidth compared to InAs dots grown directly on InP, which were successfully employed as building blocks for the first QLED operating at the C-band [13]. Finally, morphological investigations of buried QDs via TEM confirm the presence of QDs as observed via AFM, and of an homogeneous InGaAs layer, with no defects or dislocations, suggesting a very good crystal quality of all investigated samples. It is important to point out that we have tested the reproducibility of growth and optical properties of our QDs via AFM/TEM, RT-PL and μPL from tens of growths for fixed growth parameters. We did not observe significant variations among sample batches in terms of wavelength and linewidth distributions nor PL intensity, confirming that these results represent a reproducible process for fabricating such quantum dots. This work represents an important step towards the flexible use of DE in MOVPE for the fabrication of a broad range of quantum emitters in the 1.5 μm telecom window for applications in quantum photonics.

Acknowledgments

We thank Prof Richard Beanland (University of Warwick, UK) for the TEM measurements. This work has been founded by the EPSRC Grant No. EP/R03480X/1 and the InnovateUK project 'Aquasec'.

Data availability statement

The data that support the findings of this study are openly available at the following URL/DOI: https://doi.org/10.15131/shef.data.15082173.

References

[1] Gurioli M, Wang Z, Rastelli A, Kuroda T and Sanguinetti S 2019 *Nat. Mater.* **18** 799
[2] Wu J *et al* 2010 *Nano Lett.* **10** 1512
[3] Mano T, Kuroda T, Mitsuishi K, Nakayama Y, Noda T and Sakoda K 2008 *Appl. Phys. Lett.* **93** 203110
[4] Yu P, Wu J, Gao L, Liu H and Wang Z 2017 *Sol. Energy Mater. Sol. Cells* **161** 377
[5] Bimberg D, Grundmann M and Ledentsov N N 1999 *Quantum Dot Heterostructures* (Chichester: Wiley)
[6] Ledentsov N N *et al* 1996 *Phys. Rev. B* **54** 8743
[7] Steindl P, Sala E M, Alén B, Fuertes Marrón D, Bimberg D and Klenovský P 2019 *Phys. Rev. B* **100** 195407
[8] Gajjela R S R, Hendriks A L, Douglas J O, Sala E M, Steindl P, Klenovský P, Bagot P A J, Moody M P, Bimberg D and Koenraad P M 2021 *Light: Sci. Appl.* **10** 125
[9] Wang Z M, Liang B L, Sablon K A and Salamo G J 2007 *Appl. Phys. Lett.* **90** 113120
[10] Heyn C, Stemmann A and Hansen W 2009 *Appl. Phys. Lett.* **95** 173110
[11] Kim J S, Kawabe M and Koguchi N 2006 *Appl. Phys. Lett.* **88** 072107
[12] Sala E M, Bollani M, Bietti S, Fedorov A, Esposito L and Sanguinetti S 2014 *J. Vac. Sci. Technol. B* **32** 061206
[13] Müller T, Skiba-Szymanska J, Krysa A B, Huwer J, Felle M, Anderson M, Stevenson R M, Heffernan J, Ritchie D A and Shields A J 2018 *Nat. Commun.* **9** 862
[14] Anderson M, Müller T, Huwer J, Skiba-Szymanska J, Krysa A B, Stevenson R M, Heffernan J, Ritchie D A and Shields A J 2020 *npj Quantum Inf.* **6** 14
[15] Anderson M, Müller T, Skiba-Szymanska J, Krysa A B, Ritchie D A and Shields A J 2021 *Appl. Phys. Lett.* **118** 014003
[16] Sala E M, Na Y I, Godsland M, Trapalis A and Heffernan J 2020 *Phys. Status Solidi RRL* **14** 2000173
[17] Xiang Z-H, Huwer J, Skiba-Szymanska J, Stevenson R M, Ellis D J P, Farrer I, Ward M B, Ritchie D A and Shields A J 2020 *Commun. Phys.* **3** 121
[18] Senellart P, Solomon G and White A 2017 *Nat. Nanotechnol.* **12** 1026
[19] Hepp S, Jetter M, Portalupi S L and Michler P 2019 *Adv. Quantum Technol.* **2** 1900020
[20] Stevens M A, Tomasulo S, Maximenko S, Vandervelde T E and Yakes M K 2017 *J. Appl. Phys.* **121** 19
[21] Noda T, Mano T, Jo M, Kawazu T and Sakaki H 2012 *J. Appl. Phys.* **112** 063510
[22] Yin Z, Tang X, Sentosa D and Zhao J 2006 *Nanotechnology* **17** 1646
[23] Xiaohong T, Zongyou Y, Jinghua T, Anyan D and Koy C M 2008 *IEEE Trans. Nanotechnol.* **7** 4

[24] Hwang H, Yoon S, Kwon H, Yoon E, Kim H-S, Lee J Y and Cho B 2004 *Appl. Phys. Lett.* **85** 6383
[25] Sala E M, Godsland M, Trapalis A and Heffernan J 2021 *Phys. Status Solidi RRL* **15** 2100283
[26] University of Sheffield data repository https://doi.org/10.15131/shef.data.15082173
[27] Bugajski M and Lewandowski W 1985 *J. Appl. Phys.* **57** 521
[28] Oshinowo J, Forchel A, Grützmacher D, Stollenwerk M, Heuken M and Heime K 1992 *Appl. Phys. Lett.* **60** 2660
[29] Schliwa A, Winkelnkemper M and Bimberg D 2007 *Phys. Rev. B* **76** 205324
[30] Wang C F, Badolato A, Wilson-Rae I, Petroff P M, Hu E, Urayama J and Imamoğlu A 2004 *Appl. Phys. Lett.* **85** 3423
[31] Zhai L, Löbl M C, Nguyen G N, Ritzmann J, Javadi A, Spinnler C, Wieck A D, Ludwig A and Warburton R J 2020 *Nat. Commun.* **11** 4745
[32] Beanland R 2005 *Ultramicroscopy* **102** 115
[33] Costantini G, Rastelli A, Manzano C, Acosta-Diaz P, Songmuang R, Katsaros G, Schmidt O G and Kern K 2006 *Phys. Rev. Lett.* **96** 226106
[34] Skiba-Szymanska J *et al* 2017 *Phys. Rev. Appl.* **8** 014013